

Subscriber access provided by UNIV OF WISCONSIN - MADISON

## Agricultural and Environmental Chemistry

# Copper nanomaterial morphology and composition control foliar transfer through the cuticle and mediate resistance to root fungal disease in tomato (Solanum lycopersicum)

Yu Shen, Jaya Borgatta, Chuanxin Ma, Wade Elmer, Robert J Hamers, and Jason C. White J. Agric. Food Chem., Just Accepted Manuscript • DOI: 10.1021/acs.jafc.0c04546 • Publication Date (Web): 16 Sep 2020 Downloaded from pubs.acs.org on September 18, 2020

#### **Just Accepted**

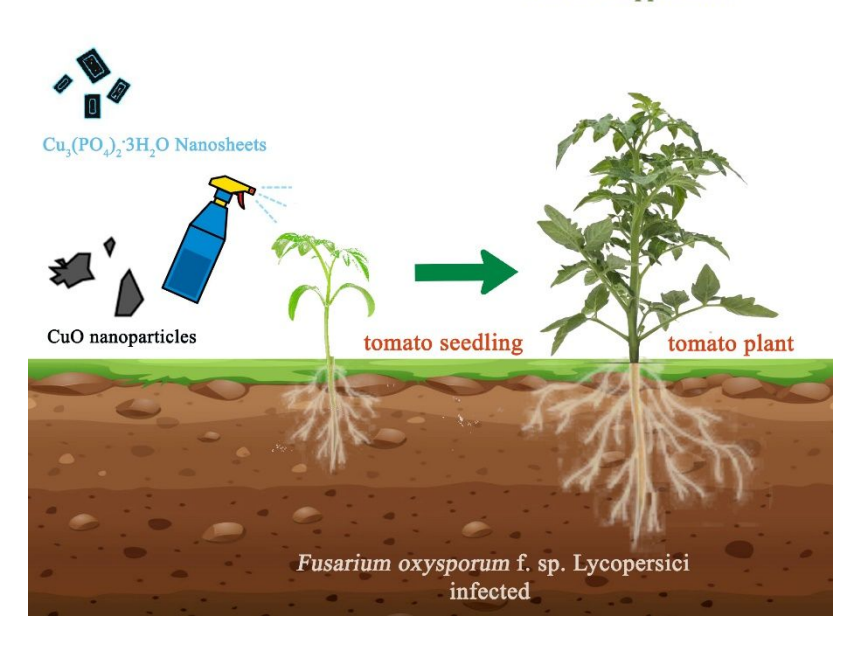
"Just Accepted" manuscripts have been peer-reviewed and accepted for publication. They are posted online prior to technical editing, formatting for publication and author proofing. The American Chemical Society provides "Just Accepted" as a service to the research community to expedite the dissemination of scientific material as soon as possible after acceptance. "Just Accepted" manuscripts appear in full in PDF format accompanied by an HTML abstract. "Just Accepted" manuscripts have been fully peer reviewed, but should not be considered the official version of record. They are citable by the Digital Object Identifier (DOI®). "Just Accepted" is an optional service offered to authors. Therefore, the "Just Accepted" Web site may not include all articles that will be published in the journal. After a manuscript is technically edited and formatted, it will be removed from the "Just Accepted" Web site and published as an ASAP article. Note that technical editing may introduce minor changes to the manuscript text and/or graphics which could affect content, and all legal disclaimers and ethical guidelines that apply to the journal pertain. ACS cannot be held responsible for errors or consequences arising from the use of information contained in these "Just Accepted" manuscripts.

1	Copper nanomaterial morphology and composition control foliar					
2	transfer through the cuticle and mediate resistance to root fungal					
3	disease in tomato (Solanum lycopersicum)					
4						
5 6	Yu Shen,† Jaya Borgatta,† Chuanxin Ma, Wade Elmer,§ Robert J. Hamers†,* and Jason C. White //,*					
7 8	<sup>†</sup> Center for Sustainable Nanotechnology, Department of Chemistry, University of Wisconsin–Madison, 1101 University Avenue, Madison, Wisconsin 53706, United States					
9 LO	§ Department of Plant Pathology and Ecology, The Connecticut Agricultural Experiment Station, 123 Huntington Street, New Haven, Connecticut 06504, United States					
l1 l2	Department of Analytical Chemistry, The Connecticut Agricultural Experiment Station, 123Huntington Street, New Haven, Connecticut 06504, United States					
L3						
L4						
L5						
<b>L</b> 6						

- Two copper nanomaterials (CuO nanoparticles [NPs] and Cu<sub>3</sub>(PO<sub>4</sub>)<sub>2</sub>·3H<sub>2</sub>O nanosheets) and 18 CuSO<sub>4</sub> were applied to tomato (Solanum lycopersicum) leaves and elemental Cu movement from 19 the leaf surface through the cuticle and into the interior leaf tissue was monitored over 8 hours. 20 21 Two forms of nanoscale Cu were used to foliar treat tomato on a weekly basis in greenhouse and 22 field experiments in the presence of the pathogen Fusarium oxysporum f. sp. lycopersici. For 23 CuSO<sub>4</sub>, Cu accumulation and retention in the cuticle was over 7-fold greater than the nanomaterials, demonstrating that nanoscale morphology and composition mediate Cu accumulation in leaf tissue. 24 25 In the greenhouse, weekly foliar applications of the nanosheets and NPs increased seedling 26 biomass by 90.9% and 93.3%, respectively, as compared to diseased and ionic Cu controls. In the field, Cu<sub>3</sub>(PO<sub>4</sub>)<sub>2</sub>·3H<sub>2</sub>O nanosheets reduced disease progress by 26.0% and significantly increased 27 fruit yield by over 45.5% per plant relative to the other treatments in diseased soil. These findings 28 suggest that nanoscale nutrient chemical properties can be tuned to maximize and control 29 30 movement through the cuticle and that interactions at the seedling leaf biointerface can lead to season long benefit for tomato growing in the presence of *Fusarium spp*. 31
- Key words: Copper nanoparticle, tomato, *Fusarium oxysporum* f. sp. *lycopersici*, Foliar application, Disease suppression
- 35

### 37 Graphical Abstract

#### Disease Suppression



38

#### INTRODUCTION

With the global population projected to reach 9.7 billion by 2050, agricultural production will need to increase by 60% or more, making maintaining global food security among the most significant challenges humanity will face. 1-3 Additional factors such as a changing climate and decreasing acreage of arable land are complicating efforts to increase food production. 4-5 We highlighted in a recent review that annual increases in production yield for the vast majority of crops have been steadily declining over the last 40 years. 6-7 Plant pathogen activity and disease also significantly reduce the marketable yield of most major crops. 8 The range of plant pathogens is incredibly diverse, including disease agents such as viruses, bacteria, fungi, oomycetes and nematodes, with most crops being impacted by multiple threats, often simultaneously .9-10 Global losses to plant disease approach an estimated \$40 billion annually, 11 with decreases of 20-40% in crop yield being typical. 12 Importantly, these losses are occurring in spite of the extensive use of pesticides in agriculture. The current level of pesticide use has raised concerns for both environmental and public health. 13-14 The development of novel and sustainable strategies for effective disease management are urgently needed and will play a central role in efforts to combat food insecurity.

Interest in the use of nanotechnology in agriculture has increased significantly in the last 5 years. <sup>15-16</sup> Much of this interest stems from the increased activity and tunability of nanomaterials as a function of nanoscale size; given the above-described inefficiencies in agriculture, the use of nanoscale platforms that afford greater control through precision agriculture could yield dramatic improvements over current practices. For example, Lui and Lal (2014) reported that application of the synthetic nanoscale hydroxyapatite (nHA) increased soybean growth rates and seed yield by 32.6% and 20.4%, respectively, as compared to amendment with a regular P fertilizer. <sup>17</sup> Ye et al. (2020) reported that 1 mg kg<sup>-1</sup> MgO nanoparticle (MgO NP)-treated *Capsicum annuum* seeds exhibited improved resistance to salinity at early stages of development. <sup>18</sup> Dimkpa et al. (2020) reported that coating urea with low-dose nanoscale ZnO promoted the overall growth of wheat and increased uptake of Zn was noted under drought stress. <sup>19</sup> In two studies from our group, we showed that foliar application of CuO nanoparticles (NPs) and Cu<sub>3</sub>(PO<sub>4</sub>)<sub>2</sub>·3H<sub>2</sub>O nanosheets could improve the growth and yield of pathogen infested watermelon and tomato in both greenhouse and field studies, with maximum disease rates being significantly reduced. <sup>20-21</sup> Importantly, the mechanism of action appears to be related to enhanced nutritional status and activated defensive

72

73

74

75

76

77

78

79

80

81

82

83

84

85

86

87

88

89

90

91

92

93

94

95

96

97

98

99

100

101

pathways by the time sensitive presence of additional Cu derived from nanoscale forms. We specifically note that there is no evidence for direct antifungal activity of the foliar added Cu against to soil-borne pathogens. Furthermore, Borgatta et al. (2018) showed that tuning material properties such as morphology (sheets vs irregular) and composition (phosphate vs oxide) led to equivalent efficacy at nearly 10-fold lower dose with infested watermelon. Ma et al. (2019) reported similar findings in a greenhouse study with tomato and was able to correlate enhanced resistance to disease with a time-dependent expression of key plant defense genes; again, this plant molecular response was sensitive to material-specific nanoscale properties.<sup>20-21</sup> The development of sustainable nanoscale platforms for disease management will require a thorough understanding of the relevant mechanisms of action, including critical chemical interactions between the nanomaterial and the leaf biointerface.

The plant leaf surface is a widespread and highly unique hydrophobic surface in the environment. The plant cuticle is a protective layer or film on leaves and other shoot tissues and consists of lipid and hydrocarbon polymers a with wax covering; the primary function of this structure is to limit water loss from the plant and to serve as an external protective barrier.<sup>22</sup> For example, it has been reported that leaf and cuticle thickness will affect the extent of damage after Titanium (Ti) application in both normal and shade conditions.<sup>23</sup> Also, plant leaf thickness is sensitive to plant hormones; exogenous methyl jasmonate improved resistance to insect herbivory more in a plant with a thicker cuticle, sunflower (*Helianthus annuus*), than in plants with a thinner cuticle; tomato (Solanum lycopersicum) and soybean (Glycine max).<sup>24</sup> The cuticle is perforated by structures known as stomata that can open and close to facilitate gas exchange that drives photosynthesis and regulates water loss.<sup>25</sup> A number of studies have investigated foliar applications of nanomaterials. For example, Arora et al. (2012) reported that foliar application of 25 mg kg<sup>-1</sup> Au NPs improved leaf number and internal redox status of treated *Brassica juncea*.<sup>26</sup> The foliar application of ZnO NP to coffee plants increased fresh root and leaf weight by 37% and 95%, respectively, when compared to controls.<sup>27</sup> Similarly, the application of 500 mg kg<sup>-1</sup> sodium tripolyphosphate (Na<sub>5</sub>P<sub>3</sub>O<sub>10</sub>, STP) NP to tomato increased fruit production by 207%.<sup>28</sup> As noted above, our group has published a number of studies demonstrating the efficacy of nanoscale foliar Cu and Si amendments to increase disease tolerance and yield. <sup>20-21, 29</sup> The cuticle is a bridge between the outer environment and internal plant tissues, including vascular structures, and the mechanisms by which NPs cross this unique hydrophobic surface will be critical to effects

designed to improve plant growth and disease resistance in agriculture. Although a number of studies have investigated and demonstrated the potential efficacy of the foliar application of nanomaterials, few have sought to understand the pathway of entry from the leaf surface into the plant, as well as the role of nanomaterial and cuticle properties in mediating that process of uptake and conveyed plant benefit.

This study includes a mechanistic investigation of the transfer of nanoscale and ionic forms of Cu from the tomato leaf surface to the cuticle and into interior leaf tissue over an 8-hour period. In addition, greenhouse and field experiments were conducted to investigate the role of Cu sources (nanoscale, ionic), morphology (irregular, nanosheet), and composition (oxide, phosphate) on the efficacy of Cu to modulate plant nutrition and increase resistance to fungal infection. Importantly, multiple applications were made to both greenhouse- and field-grown plants to maximize benefit. At harvest, physiological parameters including disease progress, biomass and pigment content were evaluated. The tissue content of essential nutrients and pathogen-related enzymes activities were measured to characterize the underlying mechanism of plant response. These findings add to our understanding of how nanoscale chemical interactions at the leaf biointerface control Cu accumulation, modulate plant nutrition and stimulate resistance to *Fusarium spp.*, and advance efforts to sustainably employ nanotechnology in agriculture.

#### MATERIALS AND METHODS

Research Nanomaterials (Houston TX). Cu<sub>3</sub>(PO<sub>4</sub>)<sub>2</sub>•3H<sub>2</sub>O nanosheets were synthesized and characterized as reported previously.<sup>20</sup> Copper chloride dihydrate, ammonium phosphate monobasic, and diethylene glycol were obtained from Sigma Aldrich (St. Louis MO).<sup>30-31</sup> All reagents were used as purchased. For all plant exposure experiments, the CuO nanoparticles (NP) and Cu<sub>3</sub>(PO<sub>4</sub>)<sub>2</sub>•3H<sub>2</sub>O nanosheets were applied by mass concentration (mg L<sup>-1</sup>) but were adjusted based on the actual amount of added Cu. Quantitative measurements using inductively coupled plasma mass spectrometry verified that the stoichiometries of CuO and Cu<sub>3</sub>(PO<sub>4</sub>)<sub>2</sub>•3H<sub>2</sub>O materials

contain  $85 \pm 6\%$  and  $44 \pm 4\%$  mass percent of Cu, respectively. <sup>20-21</sup>

Material Characterization. Nanoscale CuO (30 nm diameter; powder) was purchased from U.S.

132

133

134

135

136

137

138

139

140

141

142

143

144

145

146

147

148

149

150

151

152

153

Cuticle Cu Extraction. As noted above, the plant cuticle is a complex mixture of cutin, polysaccharides, waxes, phenolic compounds, among other constituents. It is known that nitric acid can dissolve the cuticle on the leaf surface; 32-33 as such, experiments were conducted to measure the movement of foliar applied nanoscale and ionic Cu from the leaf surface through the cuticle and into the leaf interior tissues. Specifically, after foliar application of nanoscale Cu (both CuO NPs and Cu<sub>3</sub>(PO<sub>4</sub>)<sub>2</sub>•3H<sub>2</sub>O nanosheets) and CuSO<sub>4</sub>, 35% nitric acid was used to extract and isolate the cuticle over the course of 8 hours. Specifically, we isolated the following fractions over time: (1) DI water (Millipore Milli-Q® water purification system) was used to wash the outer surface of the leaf for 5 min, and the collected rinsate is denoted as the "surface attached" fraction; (2) the rinsed leaves were then transferred into the 35% nitric acid for 15 min; we refer to the collected nitric acid as the "cuticle" fraction; and (3) the rinsed- and cuticle-free leaf was then digested in concentrated nitric acid to isolate the "interior leaf" accumulated Cu fraction (Figure S1). Copper from outer surface washing and interior tissues was quantified using inductively coupled plasma optical emission spectroscopy (ICP-OES) on a Thermo Fisher iCAP 6500 (Thermo Fisher Scientific, Waltham, MA); the cuticle fraction was measured by ICP with mass spectrometry (ICP-MS) on an Agilent 7500ce (Agilent, Santa Clara, CA)(due to lower Cu content). Importantly, the nutrient Mg is used as a biomarker to insure minimal whole leaf damage during cuticle removal; specifically, presence of Mg in the cuticle fraction indicates significant leaf damage and contamination of the cuticle fraction with interior leaf constituents (including Cu). For this experiment, we foliar sprayed 50 mg L<sup>-1</sup> Cu<sub>3</sub>(PO<sub>4</sub>)<sub>2</sub>•3H<sub>2</sub>O nanosheets, 31.25 mg L<sup>-1</sup> CuO NPs, and 62.50 mg L<sup>-1</sup> CuSO<sub>4</sub> solution on tomato leaves of separate replicate plants, and collected the tomato leaf fractions noted above at intervals of 2, 4, 6 and 8 h. In this experiment, we have 12 individual replicate plants at 4 time points, with three replications for each treatment.

154

155

156

157

158

159

160

Greenhouse Experiment and Field Experiment. For the greenhouse and field experiments, tomato (*Solanum lycopersicum* L. cv Bonnie Best [a commonly grown variety that is susceptible to Fusarium wilt]; Harris Seed Co., Rochester NY) seeds were germinated in 36 cell (5.66 × 4.93 × 5.66 cm) plastic liners (1 plant per cell) filled with soilless potting mix (ProMix BX. Premier Hort Tech, Quakertown, PA, USA). After three weeks, the seedlings were fertilized with 40 ml of Peter's soluble 20-10-20 (N-P-K) fertilizer (R.J. Peters, Inc., Allentown, PA). The *Fusarium* 

oxysporum f. sp. lycopersici pathogen inoculum was prepared as described previously.<sup>34</sup> Briefly, distilled water was added to Japanese millet (1:1, wt: wt) and the mixture was autoclaved for 1 hour on two consecutive days. Agar plugs were then seeded with *F. oxysporum* f. sp. lycopersici. After culturing for 2 weeks at 22-25 °C, the millet was air-dried and ground in a mill. The inoculum was then hand incorporated into potting mix BX (without mycorrhizae; Premier Hort. Tech, Quakertown, PA, USA) at 0.75 g millet inoculum/L potting mix prior to seedling addition.

161

162

163

164

165

166

167

168

169

170

171

172

173

174

175

176

177

178

179

180

181

182

183

184

185

186

187

188

189

Uniformly sized plants with 3-4 leaves were selected for both greenhouse and field experiments. For both types of experiments, there were five treatments in both diseased and healthy soils: 1) untreated control, 2) 50 mg L<sup>-1</sup> Cu<sub>3</sub>(PO<sub>4</sub>)<sub>2</sub>•3H<sub>2</sub>O nanosheets, 3) 31.25 mg L<sup>-1</sup> CuO NPs, 4) 62.5 mg L<sup>-1</sup> CuSO<sub>4</sub> solution; 5) 42.5 mg L<sup>-1</sup> Na<sub>3</sub>(PO<sub>4</sub>) solution. Nanoscale suspensions of Cu<sub>3</sub>(PO<sub>4</sub>)<sub>2</sub>•3H<sub>2</sub>O nanosheets or CuO nanoparticles were prepared in deionized (DI) water amended with a nonionic surfactant (Regulaid® 1 mL L<sup>-1</sup>); this type of surfactant is typical in commercial agrichemical formulations and facilitates material retention on the leaves.<sup>20</sup> The CuO suspension was sonicated with probe sonicator for 2 min in an ice bath. Because of concern over possible material breakage, the Cu<sub>3</sub>(PO<sub>4</sub>)<sub>2</sub>•3H<sub>2</sub>O nanosheets were sonicated using a gentler procedure; the suspension was 500-watt bath sonicated via ultrasonic processor probe (Cole-Parmer, Vernon Hills, IL) for 1 min. A "dip application" was used for treatment; each plant was inverted into the suspension for approximately 5 seconds, resulting in a dose of approximately 1.8 mL of suspension as measured by solution volume difference before and after immersion. The solutions were redispersed after treatment of 11 plants for the greenhouse experiment and after 4 plants for the field experiment (a function of different replicate numbers). The plants were then inverted and allowed to dry for 1 hour. For the greenhouse experiment, the seedlings were transplanted into 10 cm diameter plastic pots (350 mL) containing potting mix that was infested with Fusarium spp. or not infested. A foliar application of the nanoparticles was made once per week during the 4-week growth period.<sup>34</sup> The tomato seedlings were arranged on greenhouse benches in a randomized block design. Temperatures averaged 17-22 °C night and 19-25 °C day. Select replicate tomato seedlings were harvested every 7 days for during the 28-day growth period (4 harvests). At harvest, measured endpoints included biomass, phenotypic appearance, disease progress (AUDPC; see below), and elemental content.

For the field experiment, potted tomato seedlings were transplanted at the Connecticut Agricultural Experiment Station Lockwood farm in Hamden, Connecticut. A plot distribution map for the tomato seedlings by treatment is shown in Figure S2. Fertilizer (10-10-10, N-P-K) was spread over a 0.9 m wide rows at a rate of 112 kg per ha. The rows were set 1.5 m apart, covered in black plastic mulch and lined with irrigation drip tape. Plants were cultivated over the summer; disease progress was monitored during the growth period and harvested tomato fruit mass was recorded at day 83 and destructive harvest occurred on day 97. The measured endpoints included phenotypic characteristics, biomass, disease progression (quantified via Area Under the Disease Progress Curves, AUDPC, as described below), and the elemental composition of tomato tissues.

**AUDPC Calculation.** Plants were rated for severity of fungal disease on a scale of 1 to 5 where 1 = no disease, 2 = slightly stunted, 3 = stunted and or partially wilted, 4 = completely wilted, and 5 = dead.<sup>35</sup> Disease progress was determined by plotting the cumulative ratings from replicate plants over time and then calculating the AUDPC using the trapezoid rule, where  $Y_i$  = the disease rating at time  $t_i$ ,

205 
$$AUDPC = \sum [Y_i + Y_{(i+1)}]/2 \times (t_{(i+1)} - t_i)$$
 (1)

Tissue Element Analysis. Root and shoot tissue from greenhouse and field experiments, as well as fruits from the field studies, were dried in an oven at 50 °C, ground in a Wiley mill, and passed through a 1 mm sieve. One tomato fruit from each field plot was randomly selected and assayed to determine the concentration of Cu and other nutrients. Digestion of ground samples (0.5 g) was done in 50 mL polypropylene digestion tubes with 5 mL of concentrated nitric acid at 115 °C for 45 min on a hot block (DigiPREP System; SCP Science, Champlain, NY). The content of Ca, Cu, Fe, K, Mg, Mn, P, and Zn was determined by inductively coupled plasma optical emission spectroscopy (ICP-OES) on a Thermo Fisher iCAP 6500 (Thermo Fisher Scientific, Waltham, MA). Element content was expressed as μg g-¹ (dry weight) plant tissue. Yttrium (Yi) was used as an internal standard and a sample of known concentration was analyzed every fifteen samples. The Quality Control Standard (QCS) and Certified Reference Materials were purchased from SPEX

CertiPrep (Metuchen, NJ) and included QCS 21 for Ca, Cu, Fe Mg, Mn and Zn, QCS 7 for K and Single-Element of Phosphorus (P) Standard as certified reference materials.

220

229

- 221 Plant Defense Enzyme Activity and Protein Content For the greenhouse experiments, the activity of phenylalanine ammonia lyase (PAL), peroxidase (POD) and polyphenol oxidase (PPO), 222 223 as well as the total protein content, was determined the root tissue of tomato seedlings from the 224 different treatments. One gram of fresh tomato root tissue was ground with a mortar and pestle in liquid nitrogen. The resulting powder was macerated in 4 ml of ice-cold 50 mM potassium 225 phosphate buffer (pH 6.8) containing 1 % polyvinylpyrrolidone (PVP), 1 mM ethylene diamine 226 tetra-acetate (EDTA). The homogenates were centrifuged at 8,000 rpm at 4 °C for 30 min. The 227 228 supernatants (crude enzyme extract) were immediately used for determination of POD, PPO and
- using a SpectraMax M2 Microplate Reader (Molecular Devices, LLC, San Jose, CA).
- The total protein content of the samples was quantified according to the method described by

PAL enzyme activities and total protein determination. In each case, three replicates were analyzed

- Bradford (1976).<sup>36</sup> Sample protein content was expressed as equivalent microgram bovine serum
- albumin (BSA) per 0.1 ml sample protein (μg mL<sup>-1</sup>) as determined from a standard curve of BSA
- versus absorbance.
- PAL activity (EC 4.3.1.24) was measured by the method of Mori et al. (2001) with modifications.
- 236 <sup>37</sup> A reaction mixture was prepared by adding 0.4 mL of 100 mM Tris-HCl buffer (pH 8.8) and 0.2
- 237 ml of 40 mM phenylalanine to 0.2 ml of enzyme extract. Conversion of L-phenylalanine to
- cinnamic acid at 37 °C was measured at 290 nm by reading the extract every 30 s for 5.5 min after
- 239 the start of the reaction. The enzyme activity was calculated employing a molar extinction
- 240 coefficient of 10,900 M<sup>-1</sup> cm<sup>-1</sup>.
- The activity of POD (EC 1.11.1.7) was determined by the method described by Choudhary (2011)
- with some modification.  $^{38}$  First,  $^{25}$   $\mu L$  of the crude-extract preparation was added to  $^{2}$  mL of a
- solution containing 50 mM potassium phosphate buffer (pH 6.8), 1 % guaiacol and 1 % hydrogen
- peroxide. The absorbance readings were taken at 436 nm in every 30 s for 5 min. The enzyme
- activity was calculated employing molar extinction coefficient of 26.6 mM<sup>-1</sup> cm<sup>-1</sup>.

The activity of PPO (EC 1.10.3.2) was determined by the method of Cavalcanti et al. (2007) with some modification.<sup>39</sup> The reaction mixture contained 50 µl of the crude extract, 3 ml of a solution containing 100 mM potassium phosphate buffer (pH 6.8) and 25 mM catechol. The increase in absorbance at 410 nm was measured for 10 min at 30 °C. A value of 1, 300 M<sup>-1</sup> cm<sup>-1</sup> was employed for the molar extinction coefficient of *o*-Quinone.

**Pigment Analysis.** Chlorophyll content was determined by the method of Stober and Lichtenthaler, with modification. <sup>40</sup> Briefly, 50 mg of fresh tissue was harvested, cut into pieces (<1 cm) and added to 15 mL centrifuge tubes amended with 10 mL of 95% ethanol. The tubes were kept in the dark for 3-5 d, and the chlorophyll content was measured by SpectraMax M2 Microplate Reader (Molecular Devices, LLC, San Jose, CA). For three replicates per treatment, the concentration of chlorophyll a (Chl *a*), chlorophyll b (Chl *b*) and total chlorophyll were determined by the following equations:

259 Chl 
$$a = 13.36A_{664.2} - 5.19A_{648.6}$$
 (2);

260 Chl 
$$b = 27.43A_{648.6} - 8.12A_{664.2}$$
 (3);

Total chlorophyll = 
$$Chl a + Chl b$$
 (4).

**Statistical Analysis.** Biomass, elemental content, and physiological indices were analyzed using one-way ANOVA with the three (greenhouse experiment) and five (field experiment) replications as main effects. All data except the cuticle experiment are expressed on a dry weight basis; because of the difficulty in drying nitric acid washed leaves, fresh mass was used for results in the cuticle isolation work. Means were separated using Duncan's Significant Difference Test at p < 0.05. All analyses were performed using SPSS 25 (IBM, USA).

#### **RESULT AND DISCUSSION**

#### **Cuticle Isolation Experiment.**

The Cu content in three leaf fractions was determined; the Cu content of the surface wash fraction ranged from 21.57 to 39.20 mg kg<sup>-1</sup> for the different Cu sources. Interestingly, the amount of Cu varied significantly as a function of form; the (Cu<sub>3</sub>(PO<sub>4</sub>)<sub>2</sub>•3H<sub>2</sub>O nanosheets yielded the greatest Cu content at 39.20 mg kg<sup>-1</sup>, followed by CuSO<sub>4</sub> at 27.71 mg kg<sup>-1</sup> and CuO NP at 21.57 mg kg<sup>-1</sup> at 2 h (Figure 1-a). As for the surface wash and tissue fractions at 2 h, the cuticle Cu content ranged from 10.61-17.41 mg kg<sup>-1</sup> and did not vary as a function of Cu source. The Cu content of the interior leaf fraction at 2 h was quite low, ranging from 2.02 to 2.22 mg kg<sup>-1</sup> and similar to the cuticle, did not vary as a function of Cu type. Over the next 6 h in the surface wash fraction, the amount of Cu decreased steadily and significantly over time for all Cu types, with reductions ranging from 89-99% (Figure 1a). Specifically, by 8 h the amount of Cu in the surface fraction had declined to 0.31, 0.88 and 3.14 mg kg<sup>-1</sup> for Cu<sub>3</sub>(PO<sub>4</sub>)<sub>2</sub>•3H<sub>2</sub>O nanosheets, CuO NP, and CuSO<sub>4</sub>, respectively (significantly different p<0.05).

Not surprisingly, the time-dependent decrease in Cu in the surface-wash fraction was associated with time-dependent increases in the Cu content of the cuticle and interior leaf fractions (Figure 1b, c). By 8 h, the Cu content in the cuticle had increased to 34.9, 10.7 and 255.7 mg kg<sup>-1</sup> for the Cu<sub>3</sub>(PO<sub>4</sub>)<sub>2</sub>•3H<sub>2</sub>O nanosheets, CuO NP, and CuSO<sub>4</sub>, respectively (significantly different p<0.05). This was also accompanied by Cu increases in the interior leaf fraction, where amounts at 8 h were 4.38, 4.94 and 3.61 mg kg<sup>-1</sup> for the Cu<sub>3</sub>(PO<sub>4</sub>)<sub>2</sub>•3H<sub>2</sub>O nanosheets, CuO NP, and CuSO<sub>4</sub>, respectively (significantly different p<0.05). The relative retention of Cu from ionic exposure in the cuticle fraction relative to the two nanoscale treatments is notable. This is particularly evident when the data for each fraction is normalized to the amount present in the cuticle fraction at 2 hours (Table 1). At 2, 4, 6 and 8 h, the relative amount of Cu present in the cuticle fraction is 1.0, 1.33, 1.60, and 2.01 for CuO NPs; the values for the Cu<sub>3</sub>(PO<sub>4</sub>)<sub>2</sub>•3H<sub>2</sub>O nanosheets are 1.0, 1.22, 1.67, and 0.85. However, for the ionic form, the relative amounts the cuticle at 2, 4, 6, and 8 h were 1.0, 1.87, 15.77 and 24.10.

From the data, it is clear that Cu derived from nanoscale forms can pass more quickly through the cuticle than the ionic sulfate form. In addition, it is also clear that more Cu moves through the cuticle and into the leaf when the nanoscale foliar application is with Cu<sub>3</sub>(PO<sub>4</sub>)<sub>2</sub>•3H<sub>2</sub>O nanosheets as compared to CuO NPs. The foliar application of nanoparticles has been widely used in the literature for a number of purposes, <sup>21,41</sup> although the mechanisms of attachment and accumulation

303

304

305

306

307

308

309

310

311

312

are largely unknown. For example, our group has shown previously and, in this report, (see below) that nanoscale foliar applications of Cu can impact element content and pathogen activity in the roots; the precise form of Cu as it accumulates in the leaves and is transported to the roots is unknown. For a foliar exposure of 100 mg L<sup>-1</sup> Ag, Zhang et al. (2018) demonstrated that the transfer ratio for Ag NPs into leaf tissue was significantly greater than the ionic form in cucumber; <sup>42</sup> these findings align well with our current results with Cu. Moreover, Larue et al. (2014) reported that TiO<sub>2</sub> NPs could be internalized inside lettuce leaves after foliar exposure of 12.5 mmol L<sup>-1</sup> TiO<sub>2</sub> NPs, and importantly, the chemical form was not changed during this process.<sup>41</sup> Additional research is needed to clarify the precise mechanism of Cu movement through the various leaf tissues, including the role and kinetics of particle transformation processes such as dissolution and corona formation.

313

314

315

316

317

318

319

320

321

322

323

324

325

326

327

328

329

330

#### **Greenhouse Experiment.**

A 4-week greenhouse experiment was conducted to compare the disease suppression efficacy of different Cu based nanomaterial treatments applied initially by dip application with three subsequent weekly foliar spray applications. At four weeks, the presence of the fungal pathogen in the soil decreased the growth of tomato by 53.3% (Figure 2a,3a). However, in the soil infested with the pathogen, the nanoscale foliar treatments significantly reduced disease progress as measured by AUDPC, with the two nanoscale treatments being the most effective (Figure S3a). The ionic P and Cu treatments reduced disease progress by approximately 17% and 19%, respectively; CuO NP applications reduced disease by approximately 40%. The Cu<sub>3</sub>(PO<sub>4</sub>)<sub>2</sub>•3H<sub>2</sub>O nanosheets were the most effective at suppressing disease, with infection being reduced by nearly 56%. Similarly, nanoscale amendments significantly increased plant biomass under diseased conditions, with the two nanoscale treatments having the greatest benefit, with significant increases of 91-93% than the diseased control (Figure 3a). Importantly, both nanoscale Cu materials resulted in significantly greater plant biomass in the diseased condition than did equivalent amendments of ionic Cu; in fact, the CuSO<sub>4</sub> treatment did not significantly increase growth relative to diseased controls. Under the healthy conditions, the repeated nanoscale foliar amendments had no impact on plant biomass (Figure 3b).

Leaf and root samples were collected every 7 days and were subjected to elemental analysis (Figure 4). The leaf Cu content of untreated shoots in the healthy plants ranged from 4.8 to 10.8 mg kg<sup>-1</sup> (Figure 4d). Not surprisingly, weekly foliar treatments with Cu in different forms significantly increased the leaf Cu content, with values being highest in the early weeks and then decreasing from growth dilution. Interestingly, the trend for the untreated controls and the ionic P treatment was reversed, although the overall levels were lower. There were some specific trends and statistically significant differences in leaf Cu content as a function of treatment type over time. At T1, the Cu content was statistically equivalent across the three Cu treatments, with values ranging from 30-38 mg kg<sup>-1</sup>; although nominally the Cu content from the Cu<sub>3</sub>(PO<sub>4</sub>)<sub>2</sub>•3H<sub>2</sub>O nanosheets was highest, with ionic Cu in the middle and the NP the lowest. By T4, the values ranged from 17-22 mg kg<sup>-1</sup>; here, the trend has reversed, with the nanoscale materials having lower nominal amounts than the ionic Cu, although only CuO NPs were significantly reduced. In the healthy plants, the Cu content of plant roots gradually increased over time across all treatments but at harvest, the levels did not differ as a function of Cu treatment type (Figure 4c); at harvest, root Cu content ranged from 20-30 mg kg<sup>-1</sup> across all treatments. However, the Na<sub>3</sub>PO<sub>4</sub> treatment was significantly lower than the control and nanoscale Cu treatments.

In the diseased plants, the trends in shoot Cu content over time were similar to the healthy controls; treated plants had higher Cu content (22-45 mg kg<sup>-1</sup>) that decreased over time to 15-28 mg kg<sup>-1</sup> (Figure 4b); the untreated controls and P ionic control had much lower levels at T1 (< 5 mg kg<sup>-1</sup>) that increased over time to approximately 10 mg kg<sup>-1</sup>. At T1, there were statistically significant differences in Cu content as a function of treatment. The CuSO<sub>4</sub> treatment had the highest Cu content at 44 mg kg<sup>-1</sup>; the two nanoscale treatments had significantly less Cu, with the nanosheets yielding 35 mg kg<sup>-1</sup> and the CuO NP yielding 23 mg kg<sup>-1</sup>. By T4, the Cu leaf content of all treatments had decreased proportionately, with the ionic content being greater at approximately 28 mg kg<sup>-1</sup> and the two nanoscale treatments being lower at 15-20 mg kg<sup>-1</sup>. Similar to the healthy controls, only CuO NPs was significantly reduced from the ionic Cu controls and all Cu amended plants had significantly greater Cu content than the Cu-free controls. Similar to the leaves, the trends in Cu content in the diseased roots tracked with the healthy treatments (Figure 4a). At T1, Cu root content ranged from 12-15 mg kg<sup>-1</sup> and did not differ significantly by treatment type. At T4, there were also no statistically significant differences in root Cu content as a function of treatment. However, there was a clear trend for increased root Cu content with the nanoscale

363

364

365

366

367

368

369

370

371

372

373

374

375

376

377

378

379

380

381

382

383

384

385

386

387

388

389

390

391

foliar amendments. The root Cu content of the unamended controls, Cu<sub>3</sub>(PO<sub>4</sub>)<sub>2</sub>•3H<sub>2</sub>O nanosheets, CuO NPs, and CuSO<sub>4</sub> were 26, 30, 30 and 24 mg kg<sup>-1</sup>. With regard to the root and leaf content of other elements (Figure S5), changes as a function of disease and/or treatment were modest. We found that the presence of disease significantly increased leaf Fe content. Regarding treatments, all nanoscale foliar applications increased root Fe content, Na<sub>3</sub>PO<sub>4</sub> significantly increased root K and P content in diseased plants (relative to both untreated and treated plants), and CuSO<sub>4</sub> significantly increased root Zn content (relative to both untreated and treated plants).

The amounts of total protein and plant defense enzymes was determined in the tomato seedling roots at T4 (final harvest) as a function of disease condition and treatment (Figure 5). At final harvest, the total protein content of healthy roots was 5.08 mg kg<sup>-1</sup>; the presence of Fusarium spp. reduced protein content actually decreased this value by 13% (Figure 5a). In the healthy treatments, foliar treatment with nanoscale CuO NP significantly increased root protein content by 46.5%; the nanosheets significantly increased levels by 29.8%. In the diseased treatments, most amendments had no impact on root protein content and did not alleviate the decreases induced by disease. Only CuO NPs had a significant impact, further reducing protein content to 3.89 mg kg<sup>-1</sup>. In the diseased soil, the presence of Fusarium spp. significantly increased root PAL and POD activity by 2.2-, and 2.9-fold, respectively (Figure 5b, c). Disease increased the root PPO content by 1.5-fold (Figure 5d). In the healthy condition, root PAL and POD levels were unaffected by foliar treatments. Root PPO levels were significantly decreased by 21.2% in the CuO NP treatment and were significantly increased by 17.5% in the CuSO<sub>4</sub> treatment. In the diseased plants, the Cu nanoscale treatments significantly increased root PAL and POD content (Figure 5b-d). Specifically, Cu<sub>3</sub>(PO<sub>4</sub>)<sub>2</sub>•3H<sub>2</sub>O nanosheets increased PAL and POD content by 93.6% and 49.1% relative to the diseased controls; for CuO NPs, the increases were 66.5% and 37.4%, respectively. Root PPO content was generally decreased by nanoscale foliar treatment, although the value was only statistically significantly for CuO NP (18% reduction).

The pigment content of tomato seedling leaves was measured at harvest as a function of disease and treatment. The presence of *Fusarium spp*. decreased chlorophyll *a*, chlorophyll *b* and carotenoid content by 48.4%, 29.3%, and 34.2%, respectively. In the healthy soil, pigment production was largely unaffected by the foliar treatments. In the diseased plants, amendment with the different forms of Cu generally increased chlorophyll and carotenoid content, in several cases

nearly alleviating the decreases caused by disease. For example, Cu<sub>3</sub>(PO<sub>4</sub>)<sub>2</sub>•3H<sub>2</sub>O nanosheets and CuO NPs increased carotenoid content by 29.6% and 38.2%; these levels are statistically equivalent to the healthy controls (Figure 6c). Similar, foliar exposure to CuO NP increased chlorophyll b content by 30.0% to levels that were equivalent to the disease-free controls (Figure 6b).

Cu nanomaterials have been reported to enhance plant growth and suppress the disease in the soil.<sup>43</sup> For example, single foliar applications of Cu<sub>3</sub>(PO<sub>4</sub>)<sub>2</sub>•3H<sub>2</sub>O nanosheets or CuO NPs significantly reduced tomato seedling disease presence by an average of 31% in F. oxysporum infested soil; <sup>21</sup> a single < 2 mL amendment of a 500 mg L<sup>-1</sup> root treatment with Cu<sub>3</sub>(PO<sub>4</sub>)<sub>2</sub>·3H<sub>2</sub>O nanosheets increased biomass by nearly 261%.<sup>20</sup> Our current findings with Cu<sub>3</sub>(PO<sub>4</sub>)<sub>2</sub>•3H<sub>2</sub>O nanosheets and CuO NPs improving the tomato seedling resistance to the F. oxysporum aligns well with this previous work. Similarly, our findings of positive nanoscale Cu impacts on protein and pigment content, as well as oxidative enzyme activity, also agrees with the current literature. Sathiyabama et al reported that copper chitosan nanoparticles stimulated finger millet growth and increased the activities of the defensive enzymes PPO and POD, resulting in an induced resistance to blast disease. <sup>44</sup> It has also been reported that CuO NPs biosynthetically prepared from *Adiantum* lunulatum extract could significantly increase levels of PPO and PAL in Lens culinar when the seeds were treated with 25 mg L<sup>-1</sup>. <sup>45</sup> In our previous work, we similarly reported that the plant defense genes of watermelon and tomato seedlings could be induced by foliar application of various Cu nanomaterials.<sup>21, 29</sup> It is interesting to note that the current study included 4 separate foliar applications of the nanoscale forms of Cu but that this repeated application regime seems to offer no greater benefit (as measured by any of the parameters noted above) than does the single application early in the seedling life cycle. The reasons for this lack of a cumulative beneficial effect are currently under study but the concept of a narrow physiological window where additional Cu (in nanoscale form) exerts positive later season impact is quite intriguing.

417

418

419

420

421

392

393

394

395

396

397

398

399

400

401

402

403

404

405

406

407

408

409

410

411

412

413

414

415

416

#### Field Experiment.

A full life cycle field study was conducted to evaluate the efficacy of nanoscale foliar Cu amendments to suppress disease and enhance tomato growth (Figure 2b). After 14 weeks of growth in the field, the presence of the fungal pathogen in the soil decreased the tomato plant growth by

423

424

425

426

427

428

429

430

431

432

433

434

435

436

437

438

439

440

441

442

443

444

445

446

447

448

449

450

451

452

62.5% and fruit yield was reduced by 48.2% (Figure 3c, d). However, in the diseased soil, the nanoscale foliar treatments seemed to reduce disease progress as measured by AUDPC, with the Cu<sub>3</sub>(PO<sub>4</sub>)<sub>2</sub>·3H<sub>2</sub>O nanosheets being the most effective (Figure S3b). Notably, the high degree of variability in the diseased controls yielded a lack of statistical significance; this is not uncommon in a field study. Nominally, the ionic Cu and P treatments reduced disease progress by 17.0% and 18.9%, respectively; foliar CuO NP applications reduced disease only by 6.9%. Conversely, foliar amendment with Cu<sub>3</sub>(PO<sub>4</sub>)<sub>2</sub>·3H<sub>2</sub>O nanosheets reduced disease progress by 33.3%. Similarly, both nanoscale amendments significantly increased total plant biomass under diseased conditions; the nanosheets and CuO NPs increased growth by 45.6% and 35.8%, respectively, although again, a high degree of variability confounded statistical significance. Notably, none of the treatments had a significant impact on fruit yield. Under the healthy conditions, the repeated foliar amendments had little impact on plant biomass. The potential exception was CuO NP, which non-significantly increased the total biomass of healthy tomato plants by 25.8%; none of the treatments impacted fruit yield.

Elemental analysis was conducted on the fruit harvested after 12 weeks, as well as on roots and leaves of plants collected after 14 weeks of growth in the field (Figure 4e-g, Figure S5). The fruit Cu content were unaffected by treatment regardless of disease presence. Not surprisingly, the leaf Cu levels was increased but interestingly, only for the diseased plants. Similarly, in the roots of healthy plants, the Cu content was unaffected by foliar treatment. However, all foliar treatments increased root Cu content by 115.5% to 123.2% at harvest time. In the harvested fruit, the content several nutrients were unaffected by either disease or treatment, including Ca, Fe, Mg, and Zn (Figure S5). However, some statistically significant changes were noted. The Fe content of tomato fruit from plants amended with CuO NP was significantly less in the diseased than healthy condition, although neither value was significantly different from the untreated controls. Similarly, the K content of fruit harvested from diseased plants amended with CuSO<sub>4</sub> was significantly decreased relative to the healthy amended plants, as well as the unamended control plants. In the healthy plants, amendment with Cu<sub>3</sub>(PO<sub>4</sub>)<sub>2</sub>•3H<sub>2</sub>O nanosheets significantly decreased fruit Mn content relative to unamended controls. Last, the P content of diseased plants amended with Cu<sub>3</sub>(PO<sub>4</sub>)<sub>2</sub>•3H<sub>2</sub>O nanosheets was reduced relative to untreated controls but was not significantly different from the other treatments. The significance of these modest changes in edible tissue nutrient content is not known, although any decreases in nutritional value with treatment or disease

certainly warrant concern. For the root and leaf tissues (Figure S6), we found that the presence of disease significantly increased root K, P, and Zn content, as well as leaf Zn content, and significantly decreased leaf Mn content. With regard to treatment, nanoscale foliar applications did result in some differences between healthy and diseased plants but importantly, these changes were consistent with changes induced by disease in the absence of treatment and there were no instances where foliar amendment alleviated a disease-induced change.

The current study is the first report on the use of nanoscale Cu materials to modulate crop nutrition to increase resistance to disease at the field scale. Notably, these results do agree with the greenhouse study in this paper and others, <sup>21</sup> and also agree with published field data on the use of foliar Cu nanomaterials on other crop species. For example, CuO NPs were more effective than other metallic oxide nanoscale micronutrients on eggplant in the field, with single foliar applications leading to a 21.1% increase eggplant plant biomass in Verticillium dahlia infested soil;<sup>34</sup> both CuO NPs and Cu<sub>3</sub>(PO<sub>4</sub>)<sub>2</sub>•3H<sub>2</sub>O nanosheets decreased Fusarium spp. damage in fieldgrown watermelon; <sup>20</sup> growth with Cu-chitosan NPs amendment increased maize biomass by 0.12 to 0.16% under Curvularia leaf spot infection; and Cu NPs increased soybean crop yield up to 16% in comparison with the untreated soybean. 46 Importantly, the fact that early life stage seedling treatments or even seed treatments with nanoscale Cu offer life-cycle long benefits to field grown crops is notable. For example, Cu-chitosan NPs treated tomato seedlings were 87% more resistant to early blight and 61% more resistant to Fusarium spp. wilt treatments.<sup>47</sup> Of interest in the current field study, it is also clear that using multiple applications of the nanoscale amendments seemed to offer no benefit beyond that of a well-time single application at the early seedling stage. Moreover, our work matches well with the previous research demonstrating that the application of nanoparticles has little impact on plant fruit content, 48, 49 highlights the potential for foliar application of nanoscale nutrients in modern agriculture.

477

478

479

480

481 482

453

454

455

456

457

458

459

460

461

462

463

464

465

466

467

468

469

470

471

472

473

474

475

476

#### **Agricultural Implications.**

Taken together, the results from our greenhouse and field studies demonstrate the significant potential for early life stage nanoscale Cu treatments to suppress soil fungal infection and sustainably promote overall plant health and yield. However, some important questions remain. What are the mechanisms by which foliar applied nanoscale Cu attaches to the leaf surface and

484

485

486

487

488

489

490

491

492

493

494

495

496

497

498

499

500

501

502

503

gains entry into the interior leaf and vascular tissue? Can nanomaterial nutrients be synthesized or tuned to optimize that process of leaf entry? The findings of the current study provide information that will help to answer both of those questions. Our results clearly demonstrate that the form of Cu greatly impacts the rate and extent to which the material is either retained by the cuticle or transfers into the interior leaf tissue. Although the precise mechanisms remain unknown, it is clear that nanoscale morphology (nanosheet vs irregular) will directly impact the rate and extent of cuticular transfer. This process appears to be unrelated to Cu dissolution on the surface given that the ionic treatment resulted in the greatest amount of element retention in the cuticle over 8 hours of exposure. Importantly, these differential rates of leaf accumulation in young seedlings transfer directly to particle specific effects that endure through the life cycle. These results suggest that material properties may be further tuned to not only maximize accumulation but to also support shoot-to-root translocation processes, including possibly inducing targeted corona formation (i.e., with carbohydrates for example) that could facilitate that process. The finding that multiple weekly applications of such materials confer no additional benefit raises both practical and basic questions that are worthy of future investigation. This suggestion of a relative narrow window of early life stage opportunity for nutritional enhancement could also be used to guide the chemistry of synthesized materials, either for foliar or potentially for seed treatments. The physiological basis of this early life stage treatment effect is also an intriguing question. In summary, this study contributes to a growing body of evidence indicating that nanoscale micronutrient amendments to young seedlings can be a powerful approach in nano-enable agriculture to sustainably increase food production.

504

505

506

507

#### ASSOCIATED CONTENT

#### **Supporting Information**

The Supporting Information is available free of charge on the ACS Publications website at DOI:.

508509

510 ORCID

511 Yu Shen: 0000-0002-6599-9236.

512	Jaya Borgatta: 0000-0002-9381-6097
513	Chuanxin Ma: 0000-0001-5125-7322
514	Wade H. Elmer: 0000-0003-3308-4899
515	Robert J. Hamers: 0000-0003-3821-9625
516	Jason C. White: 0000-0001-5001-8143
517	
518	
519	ACKNOWLEDGMENTS
520	This material is based upon work supported by the National Science Foundation under Grant No
521	CHE-2001611, the NSF Center for Sustainable Nanotechnology (CSN). The CSN is part of the
522	Centers for Chemical Innovation Program. In this study, Mr. Peter Thiel supported the greenhouse
523	and field works, and Mr. Craig Musante supported the ICP-MS work, respectively.
524	
525	
526	AUTHOR INFORMATION
527	Corresponding Authors
528	*R. J. Hamers. E-mail: rjhamers@wisc.edu (Tel, Fax: 608-262-6371).
529	*J. C. White. E-mail: Jason.White@ct.gov (Tel, Fax: 203-974-8440).
530	Notes
531	The authors declare no competing financial interest.
532	
533	
534	
535	
536	REFERENCES
537 538 539	(1) West, P. C.; Gerber, J. S.; Engstrom, P. M.; Mueller, N. D.; Brauman, K. A.; Carlson, K. M.; Cassidy, E. S.; Johnston, M.; MacDonald, G. K.; Ray, D. K.; Siebert, S., Leverage points for improving global food security and the environment. <i>Science</i> <b>2014</b> , <i>345</i> (6194), 325-328.

- 540 (2) Lipper, L.; Thornton, P.; Campbell, B. M.; Baedeker, T.; Braimoh, A.; Bwalya, M.; Caron, P.;
- Cattaneo, A.; Garrity, D.; Henry, K.; Hottle, R.; Jackson, L.; Jarvis, A.; Kossam, F.; Mann, W.; McCarthy, N.;
- Meybeck, A.; Neufeldt, H.; Remington, T.; Sen, P. T.; Sessa, R.; Shula, R.; Tibu, A.; Torquebiau, E. F.,
- 543 Climate-smart agriculture for food security. *Nat. Clim. Change* **2014**, *4* (12), 1068-1072.
- White, J. C.; Gardea-Torresdey, J., Sustainable nanomaterials by design. *Nat. Nanotechnol.* **2018**,
- 545 *13* (8), 627-629.
- 546 (4) Lobell, D. B.; Gourdji, S. M., The influence of climate change on global crop productivity. *Plant*
- 547 *Physiol.* **2012,** *160* (4), 1686-1697.
- 548 (5) Gardi, C.; Panagos, P.; Van Liedekerke, M.; Bosco, C.; De Brogniez, D., Land take and food
- security: assessment of land take on the agricultural production in Europe. *J. Environ. Plann. Man.* **2014,** 550 58 (5), 898-912.
- Lobell, D. B.; Schlenker, W.; Costa-Roberts, J., Climate Trends and Global Crop Production Since
- 552 1980 Science **2016**, *333*, 616-620.
- 553 (7) Kah, M.; Tufenkji, N.; White, J. C., Nano-enabled strategies to enhance crop nutrition and
- protection. *Nat. Nanotechnol.* **2019**, *14* (6), 532-540.
- 555 (8) Servin, A.; Elmer, W.; Mukherjee, A.; De la Torre-Roche, R.; Hamdi, H.; White, J. C.; Bindraban,
- P.; Dimkpa, C., A review of the use of engineered nanomaterials to suppress plant disease and enhance
- 557 crop yield. *J. Nanopart. Res.* **2015,** *17* (2), 21.
- 558 (9) Fisher, M. C.; Henk, D. A.; Briggs, C. J.; Brownstein, J. S.; Madoff, L. C.; McCraw, S. L.; Gurr, S. J.,
- Emerging fungal threats to animal, plant and ecosystem health. *Nature* **2012**, *484* (7393), 186-94.
- 560 (10) Chakraborty, S.; Newton, A. C., Climate change, plant diseases and food security: an overview.
- 561 *Plant Pathology* **2011,** *60* (1), 2-14.
- 562 (11) Roberts, M. J.; Schimmelpfennig, D. E.; Ashley, E.; Livingston, M. J.; Ash, M. S.; Vasavada, U., The
- Value of Plant Disease Early-warning Systems: a Case Study of USDA's Soybean Rust Coordinated
- Framework,. United States Department of Agriculture, Economic Research Service 2006.
- 565 (12) Savary, S.; Ficke, A.; Aubertot, J.-N.; Hollier, C., Crop losses due to diseases and their implications
- for global food production losses and food security. *Food Security* **2012**, *4* (4), 519-537.
- Nweke, O. C.; Sanders, W. H., 3rd, Modern environmental health hazards: a public health issue
- of increasing significance in Africa. *Environ. Health Perspect.* **2009**, *117* (6), 863-870.
- 569 (14) Quiros-Alcala, L.; Mehta, S.; Eskenazi, B., Pyrethroid pesticide exposure and parental report of
- learning disability and attention deficit/hyperactivity disorder in U.S. children: NHANES 1999-2002.
- 571 Environ. Health Perspect. **2014**, *122* (12), 1336-1342.
- 572 (15) Handford, C. E.; Dean, M.; Henchion, M.; Spence, M.; Elliott, C. T.; Campbell, K., Implications of
- 573 nanotechnology for the agri-food industry: Opportunities, benefits and risks. Trends Food Sci. Tech.
- **2014**, *40* (2), 226-241.
- 575 (16) Shen, Y.; Tang, H.; Wu, W.; Shang, H.; Zhang, D.; Zhan, X.; Xing, B., Role of nano-biochar in
- attenuating the allelopathic effect from Imperata cylindrica on rice seedlings. *Environ. Sci. Nano* **2020,** *7*
- 577 (1), 116-126.
- 578 (17) Liu, R.; Lal, R., Synthetic apatite nanoparticles as a phosphorus fertilizer for soybean (Glycine
- 579 max). Sci. Rep. 2014, 4, 5686.
- 580 (18) Ye, Y.; Cota-Ruiz, K.; Hernández-Viezcas, J. A.; Valdés, C.; Medina-Velo, I. A.; Turley, R. S.; Peralta-
- Videa, J. R.; Gardea-Torresdey, J. L., Manganese Nanoparticles Control Salinity-Modulated Molecular
- Responses in Capsicum annuum L. through Priming: A Sustainable Approach for Agriculture. ACS Sustain.
- 583 Chem. Eng. **2020**, 8 (3), 1427-1436.
- 584 (19) Dimkpa, C. O.; Andrews, J.; Fugice, J.; Singh, U.; Bindraban, P. S.; Elmer, W. H.; Gardea-
- Torresdey, J. L.; White, J. C., Facile Coating of Urea With Low-Dose ZnO Nanoparticles Promotes Wheat
- 586 Performance and Enhances Zn Uptake Under Drought Stress. Front. Plant Sci. 2020, 11, 168.

- 587 (20) Borgatta, J.; Ma, C.; Hudson-Smith, N.; Elmer, W.; Plaza Pérez, C. D.; De La Torre-Roche, R.;
- Zuverza-Mena, N.; Haynes, C. L.; White, J. C.; Hamers, R. J., Copper Based Nanomaterials Suppress Root
- Fungal Disease in Watermelon (Citrullus lanatus): Role of Particle Morphology, Composition and
- 590 Dissolution Behavior. ACS Sustain. Chem. Eng. 2018, 6 (11), 14847-14856.
- 591 (21) Ma, C.; Borgatta, J.; De La Torre-Roche, R.; Zuverza-Mena, N.; White, J. C.; Hamers, R. J.; Elmer,
- 592 W. H., Time-Dependent Transcriptional Response of Tomato (Solanum lycopersicum L.) to Cu
- Nanoparticle Exposure upon Infection with Fusarium oxysporum f. sp. lycopersici. Acs Sustain. Chem.
- 594 *Eng.* **2019,** *7* (11), 10064-10074.
- 595 (22) Yeats, T. H.; Rose, J. K., The formation and function of plant cuticles. *Plant Physiol.* **2013**, *163* (1),
- 596 5-20.
- 597 (23) Hussain, S.; Iqbal, N.; Brestic, M.; Raza, M. A.; Pang, T.; Langham, D. R.; Safdar, M. E.; Ahmed, S.;
- Wen, B.; Gao, Y.; Liu, W.; Yang, W., Changes in morphology, chlorophyll fluorescence performance and
- Rubisco activity of soybean in response to foliar application of ionic titanium under normal light and
- shade environment. *Sci. Total Environ.* **2019**, *658*, 626-637.
- 601 (24) Li, C.; Wang, P.; Menzies, N. W.; Lombi, E.; Kopittke, P. M., Effects of methyl jasmonate on plant
- 602 growth and leaf properties. *J. Plant Nutr. Soil Sci.* **2018,** *181* (3), 409-418.
- 603 (25) Riederer, M.; Schreiber, L., Protecting against water loss: analysis of the barrier properties of
- 604 plant cuticles. J. Exp. Bot. **2001**, 52 (363), 2023-2032.
- 605 (26) Arora, S.; Sharma, P.; Kumar, S.; Nayan, R.; Khanna, P. K.; Zaidi, M. G. H., Gold-nanoparticle
- 606 induced enhancement in growth and seed yield of Brassica juncea. Plant Growth Regul. 2012, 66 (3),
- 607 303-310.
- 608 (27) Rossi, L.; Fedenia, L. N.; Sharifan, H.; Ma, X.; Lombardini, L., Effects of foliar application of zinc
- sulfate and zinc nanoparticles in coffee (Coffea arabica L.) plants. Plant Physiol. Biochem. 2019, 135, 160-
- 610 166.
- 611 (28) Sathiyabama, M.; Charles, R. E., Fungal cell wall polymer based nanoparticles in protection of
- 612 tomato plants from wilt disease caused by Fusarium oxysporum f.sp. lycopersici. Carbohydr. Polym.
- **2015**, *133*, 400-407.
- 614 (29) Buchman, J. T.; Elmer, W. H.; Ma, C.; Landy, K. M.; White, J. C.; Haynes, C. L., Chitosan-Coated
- 615 Mesoporous Silica Nanoparticle Treatment of Citrullus lanatus (Watermelon): Enhanced Fungal Disease
- 616 Suppression and Modulated Expression of Stress-Related Genes. ACS Sustain. Chem. Eng. 2019, 7 (24),
- 617 19649-19659.
- 618 (30) Kim, D. H.; Im, J. S.; Kang, J. W.; Kim, E. J.; Ahn, H. Y.; Kim, J., A New Synthesis Route to
- 619 Nanocrystalline Olivine Phosphates and Their Electrochemical Properties. J. Nanosci. Nanotechno. 2007,
- 620 *7* (5), 3949-3953.
- 621 (31) Wang, D.; Buqa, H.; Crouzet, M.; Deghenghi, G.; Drezen, T.; Exnar, I.; Kwon, N.-H.; Miners, J. H.;
- Poletto, L.; Grätzel, M., High-performance, nano-structured LiMnPO4 synthesized via a polyol method. J.
- 623 Power Sources **2009**, 189 (1), 624-628.
- 624 (32) Brown, D. A.; Windham, M. T.; Anderson, R. L.; Trigiano, R. N., Influence of simulated acid rain
- on the flowering dogwood (*Cornus florida*) leaf surface. *Can. J. For. Res.* **1994,** *24* (5), 1058-1062.
- 626 (33) Padgett, P. E.; Parry, S. D.; Bytnerowicz, A.; Heath, R. L., Image analysis of epicuticular damage to
- foliage caused by dry deposition of the air pollutant nitric acid. J. Environ. Monit. 2009, 11 (1), 63-74.
- 628 (34) Elmer, W. H.; White, J. C., The use of metallic oxide nanoparticles to enhance growth of
- tomatoes and eggplants in disease infested soil or soilless medium. Environ. Sci. Nano 2016, 3 (5), 1072-
- 630 1079.
- 631 (35) Elmer, W. H., Influence of Earthworm Activity on Soil Microbes and Soilborne Diseases of
- 632 Vegetables. *Plant Dis.* **2009**, *93* (2), 175-179.
- 633 (36) Bradford, M. M., A rapid and sensitive method for the quantitation of microgram quantities of
- 634 protein utilizing the principle of protein-dye binding. Anal. Biochem. 1976, 72, 248-254.

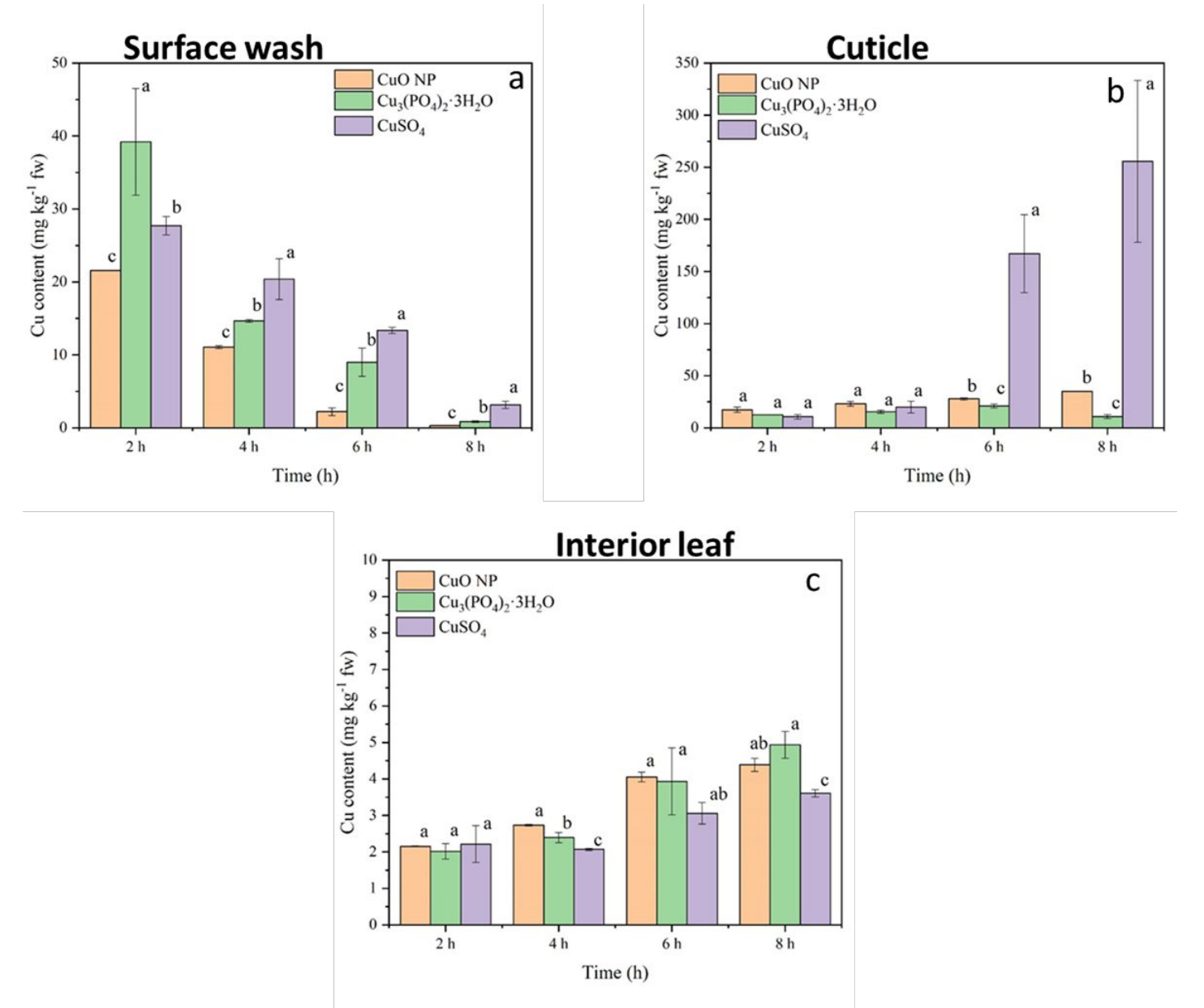
- 635 (37) Mori, T.; Sakurai, M.; Sakuta, M., Effects of conditioned medium on activities of PAL, CHS, DAHP
- 636 synthase (DS-Co and DS-Mn) and anthocyanin production in suspension cultures of Fragaria ananassa.
- 637 Plant Sci. **2001,** 160 (2), 355-360.
- 638 (38) Choudhary, D. K., Plant growth-promotion (PGP) activities and molecular characterization of
- rhizobacterial strains isolated from soybean (Glycine max L. Merril) plants against charcoal rot pathogen,
- Macrophomina phaseolina. *Biotechnol. Lett.* **2011,** *33* (11), 2287-95.
- 641 (39) Cavalcanti, F. R.; Resende, M. L. V.; Carvalho, C. P. S.; Silveira, J. A. G.; Oliveira, J. T. A., An
- aqueous suspension of Crinipellis perniciosa mycelium activates tomato defence responses against
- 643 Xanthomonas vesicatoria. *Crop Prot.* **2007**, *26* (5), 729-738.
- 644 (40) Stober, F.; Lichtenthaler, H. K., Characterization of the laser-induced blue, green and red
- fluorescence signatures of leaves of wheat and soybean grown under different irradiance. *Physiol. Plant* **1993**, *88* (4), 696-704.
- 647 (41) Larue, C.; Castillo-Michel, H.; Sobanska, S.; Trcera, N.; Sorieul, S.; Cecillon, L.; Ouerdane, L.;
- 648 Legros, S.; Sarret, G., Fate of pristine TiO2 nanoparticles and aged paint-containing TiO2 nanoparticles in
- lettuce crop after foliar exposure. *J. Hazard. Mater.* **2014,** 273, 17-26.
- 650 (42) Zhang, H.; Du, W.; Peralta-Videa, J. R.; Gardea-Torresdey, J. L.; White, J. C.; Keller, A.; Guo, H.; Ji,
- 651 R.; Zhao, L., Metabolomics Reveals How Cucumber (Cucumis sativus) Reprograms Metabolites To Cope
- with Silver Ions and Silver Nanoparticle-Induced Oxidative Stress. Environ. Sci. Technol. 2018, 52 (14),
- 653 8016-8026.
- 654 (43) Malandrakis, A. A.; Kavroulakis, N.; Chrysikopoulos, C. V., Use of copper, silver and zinc
- nanoparticles against foliar and soil-borne plant pathogens. Sci Total Environ **2019**, 670, 292-299.
- 656 (44) Sathiyabama, M.; Manikandan, A., Application of Copper-Chitosan Nanoparticles Stimulate
- 657 Growth and Induce Resistance in Finger Millet (Eleusine coracana Gaertn.) Plants against Blast Disease. J
- 658 Agric. Food Chem. **2018**, 66 (8), 1784-1790.
- 659 (45) Sarkar, J.; Chakraborty, N.; Chatterjee, A.; Bhattacharjee, A.; Dasgupta, D.; Acharya, K., Green
- 660 Synthesized Copper Oxide Nanoparticles Ameliorate Defence and Antioxidant Enzymes in Lens culinaris.
- 661 Nanomaterials-Basel **2020**, 10 (2), 312.
- 662 (46) Ngo, Q. B.; Dao, T. H.; Nguyen, H. C.; Tran, X. T.; Nguyen, T. V.; Khuu, T. D.; Huynh, T. H., Effects
- of nanocrystalline powders (Fe, Co and Cu) on the germination, growth, crop yield and product quality
- 664 of soybean (Vietnamese species DT-51). Adv. Nat. Sci. Nanosci. 2014, 5 (1), 015016.
- 665 (47) Saharan, V.; Sharma, G.; Yadav, M.; Choudhary, M. K.; Sharma, S. S.; Pal, A.; Raliya, R.; Biswas, P.,
- 666 Synthesis and in vitro antifungal efficacy of Cu-chitosan nanoparticles against pathogenic fungi of
- 667 tomato. Int. J. Biol. Macromol. 2015, 75, 346-53.
- 668 (48) Kole, C., Kole, P., Randunu, K. M., Choudhary, P., Podila, R., Ke, P. C., Rao, A. M., Marcus, R. K.
- Nanobiotechnology can boost crop production and quality: first evidence from increased plant biomass,
- fruit yield and phytomedicine content in bitter melon (Momordica charantia). BMC Biotechnol. 2013,
- 671 13(1): 37.
- 672 (49) Servin, A. D, Morales, M. I., Castillo-Michel, H., Hernandez-Viezcas, J. A., Munoz, B., Zhao, L., Nunez,
- J. E., Peralta-Videa, J. R., Gardea-Torresdey, J. L. Synchrotron verification of TiO2 accumulation in
- cucumber fruit: A possible pathway of tio2 nanoparticle transfer from soil into the food chain. *Environ*.
- 675 *Sci. Technol.* **2013,** 47, 20, 11592–11598.

677

# Figure



679



681

682 683

Figure 1 The Cu contents of the tomato leaf surface wash (a), cuticle extract (b) and tissues (c) changes in 8 h.

684 685 (Note: Bars with different letters are significantly different, and values are mean  $\pm$  S.D. (standard deviation); one-way ANOVA with Duncan's test (p < 0.05); fw, fresh weight).



Figure 2-a. Tomato seedling phenotypic response after 4 weekly foliar nanoparticle amendments.

(Note: 1, Control; 2, Cu<sub>3</sub>(PO<sub>4</sub>)<sub>2</sub> nanosheets; 3, CuO nanoparticles; 4, CuSO<sub>4</sub> solution; 5, Na<sub>3</sub>(PO<sub>4</sub>) solution; "yellow brand" indicates seedlings infested with the fungal pathogen *Fusarium oxysporum* f. sp. *lycopersici*.)



Figure 2-b. The tomato-nanoparticle field experiment biomass in both diseased and healthy soil after the harvest.

(Note: 1, Control; 2, Cu<sub>3</sub>(PO<sub>4</sub>)<sub>2</sub> nanosheets; 3, CuO nanoparticles; 4, CuSO<sub>4</sub> solution; 5, Na<sub>3</sub>(PO<sub>4</sub>) solution. "yellow number" indicates seedlings infested with the fungal pathogen *Fusarium oxysporum* f. sp. *lycopersici*.) (one-way ANOVA with Duncan's test at p < 0.05)).

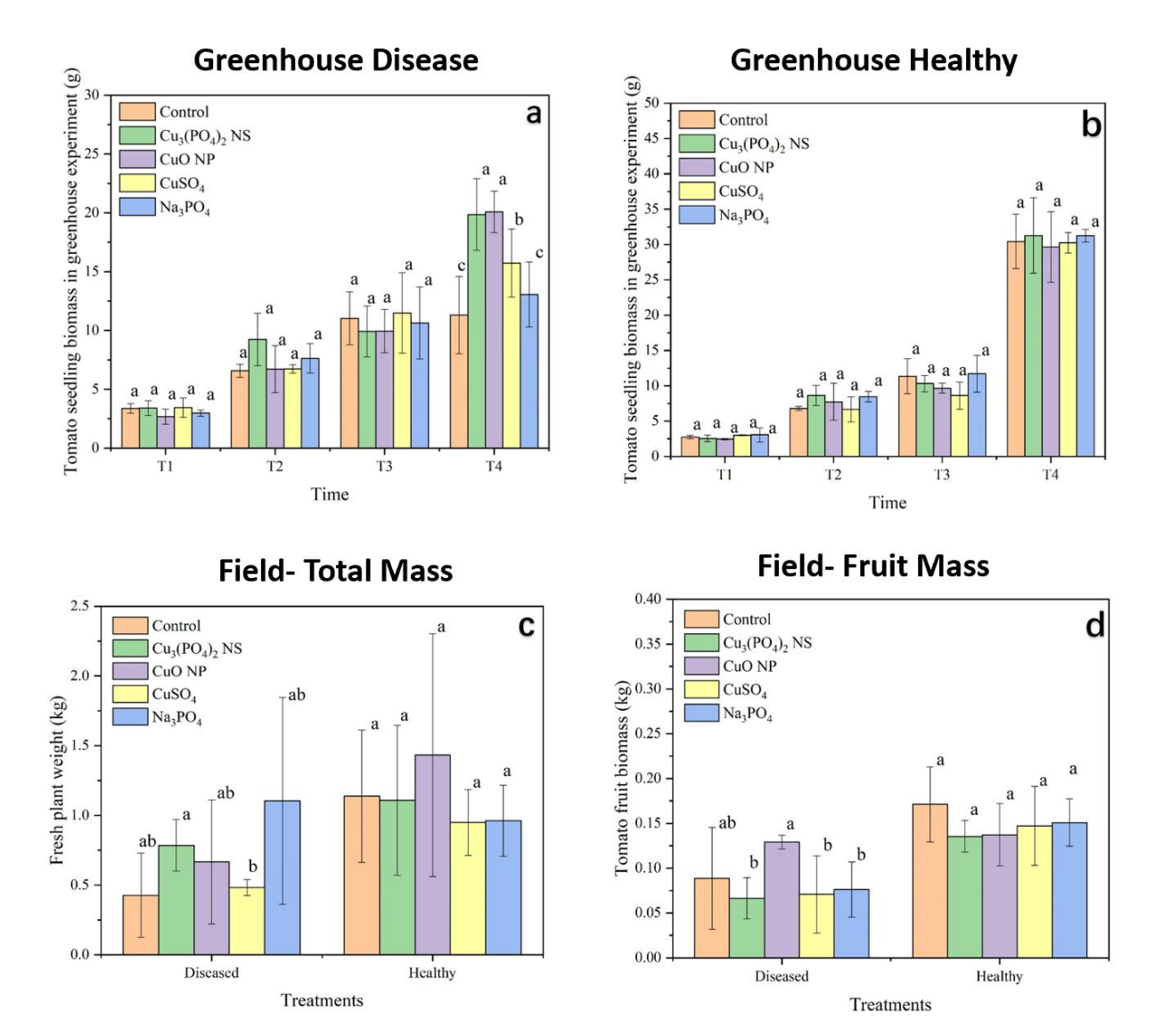
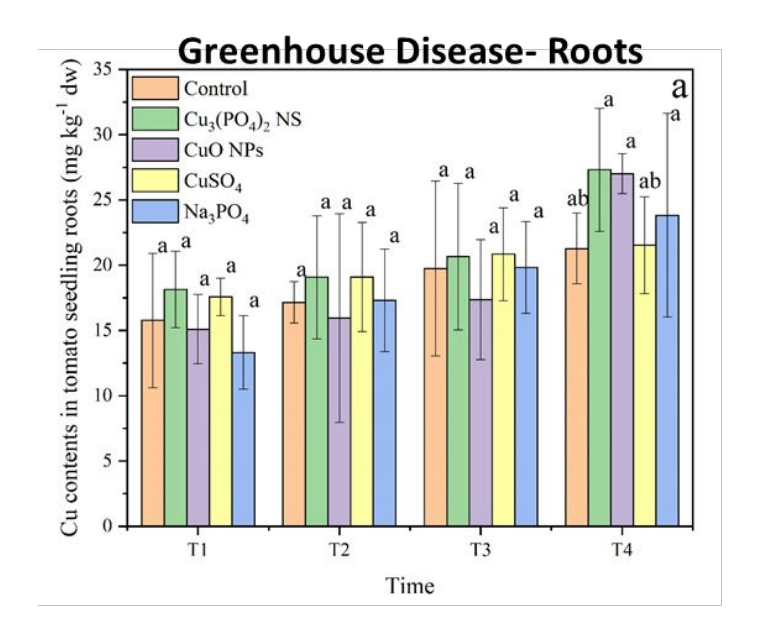
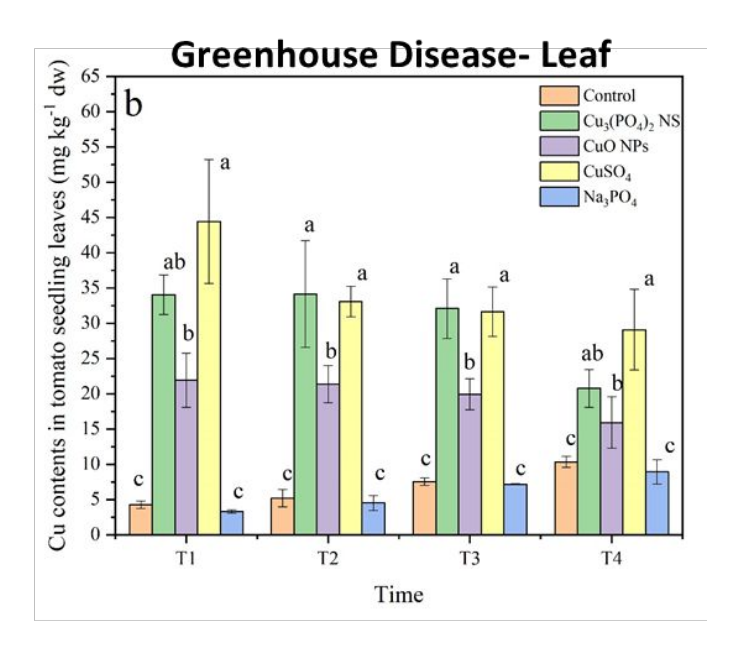
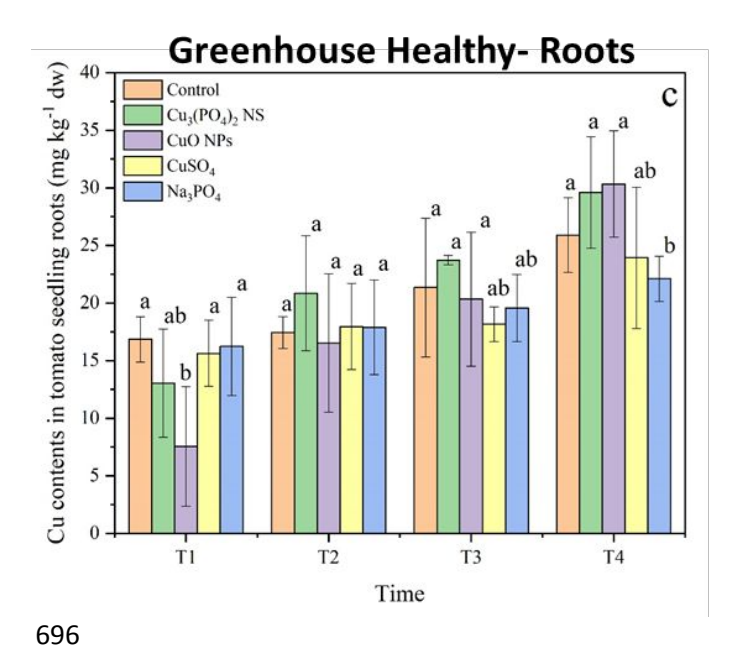


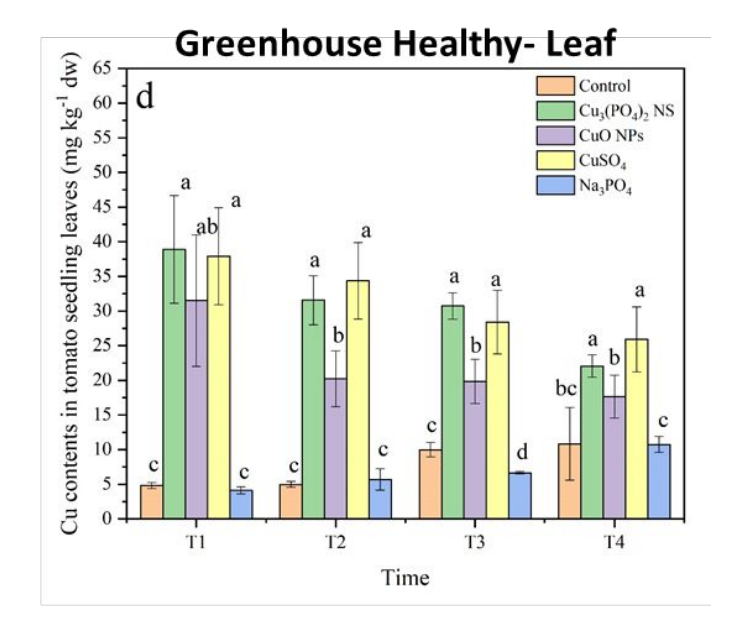
Figure 3. The biomass of the tomato seedlings in diseased (a) and healthy (b) soil in the greenhouse experiment, and the biomass of the fresh tomato plants (c) and tomato fruits (d) in the field experiment.

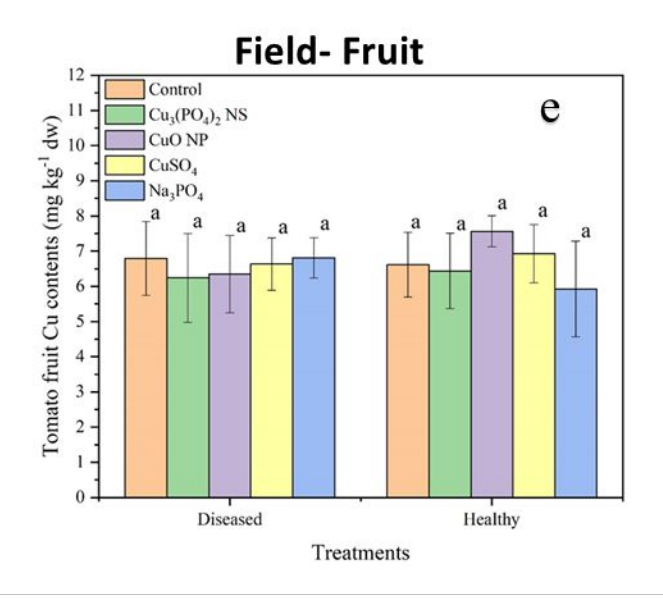
 (Note: NS, nanosheets; NP, nanoparticles; Bars with different letters are significantly different, and values are mean  $\pm$  S.D. (standard deviation); one-way ANOVA with Duncan's test (p < 0.05)).

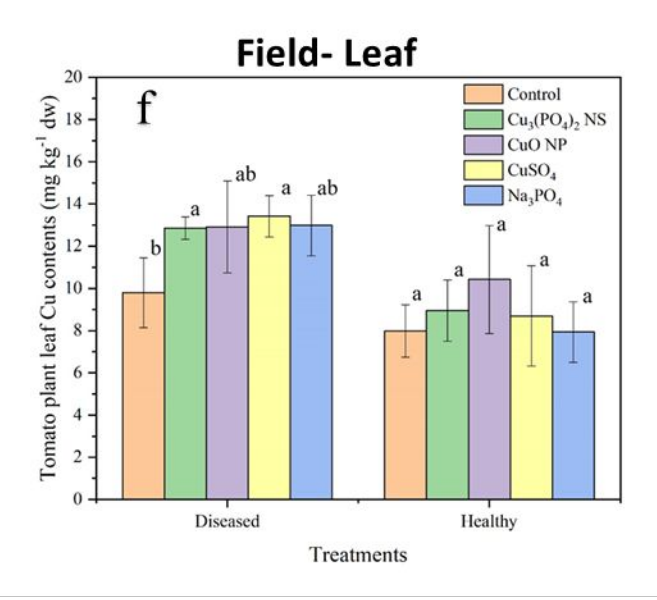


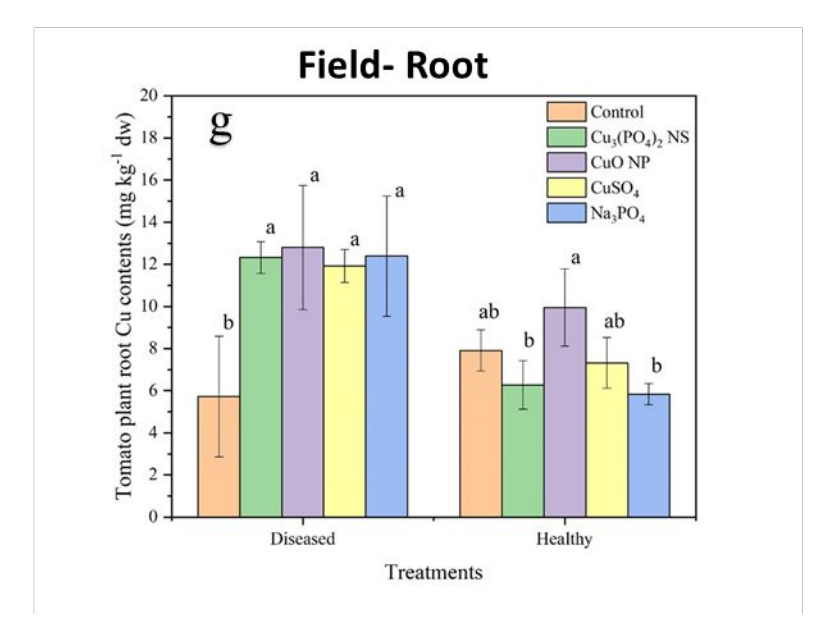












704705

706

707

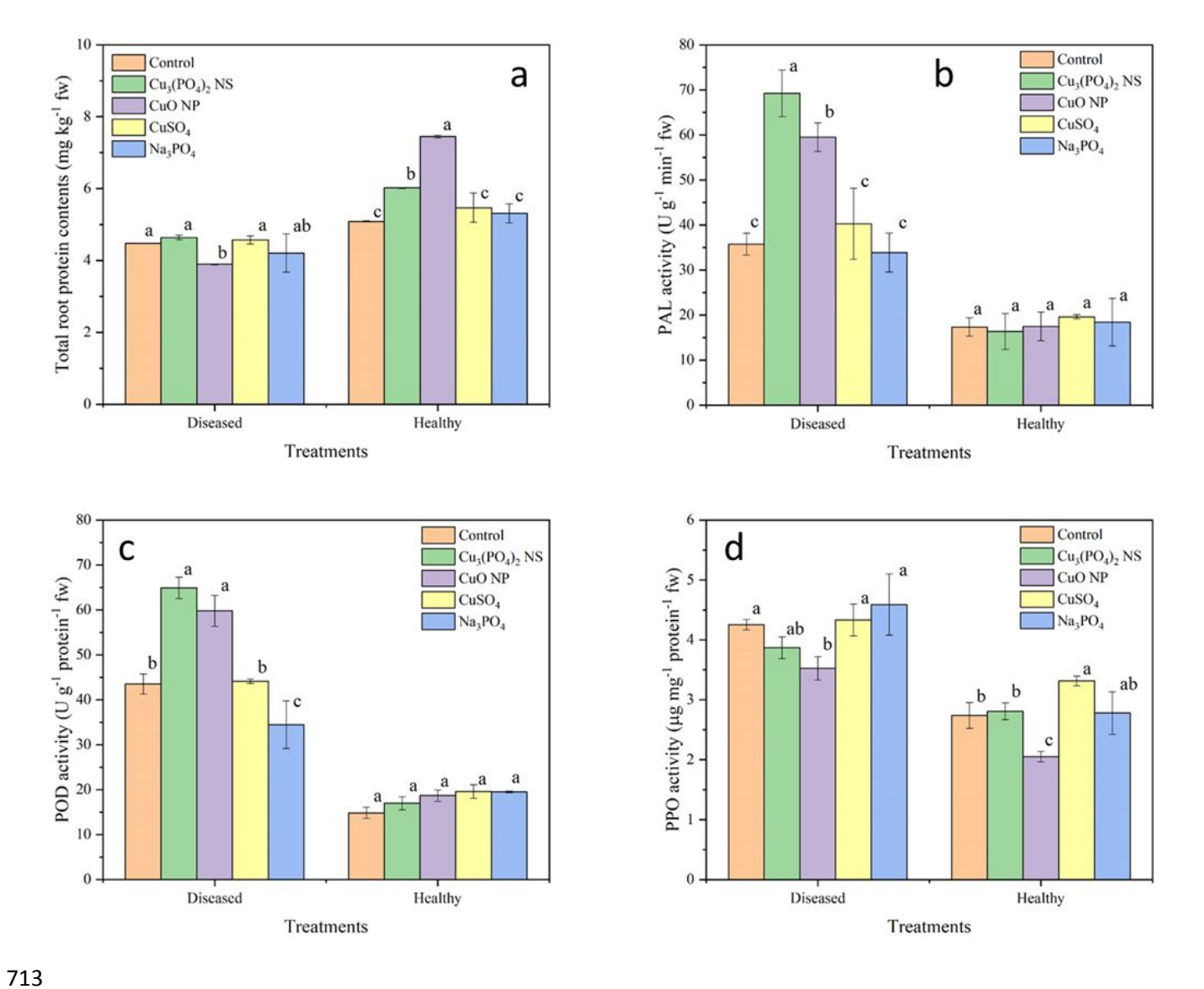
708

709

Figure 4. The Cu contents of the tomato seedlings root in diseased (a) and healthy (c) soil; and Cu contents of the tomato seedlings leaf in diseased (b) and healthy (d) soil in the greenhouse experiment, respectively; and The Cu contents of the tomato fruits (e), tomato plants leaf (f) and root (g) in the field experiment.

710711712

(Note: NS, nanosheets; NP, nanoparticles; Bars with different letters are significantly different; one-way ANOVA with Duncan's test (p < 0.05), and values are mean  $\pm$  S.D. (standard deviation); dw, dry weight; T means weekly harvest time).



715

716

717

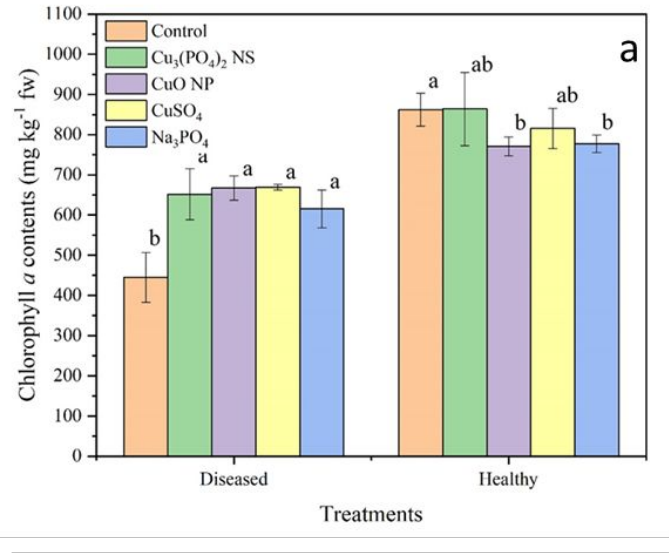
718

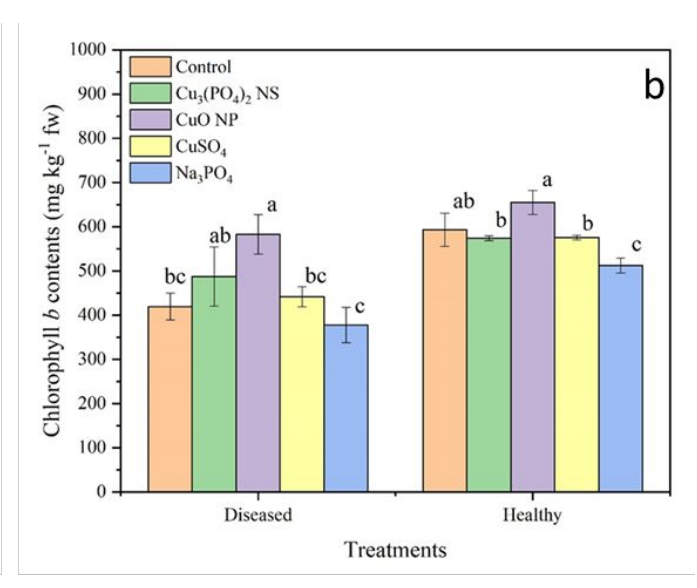
719

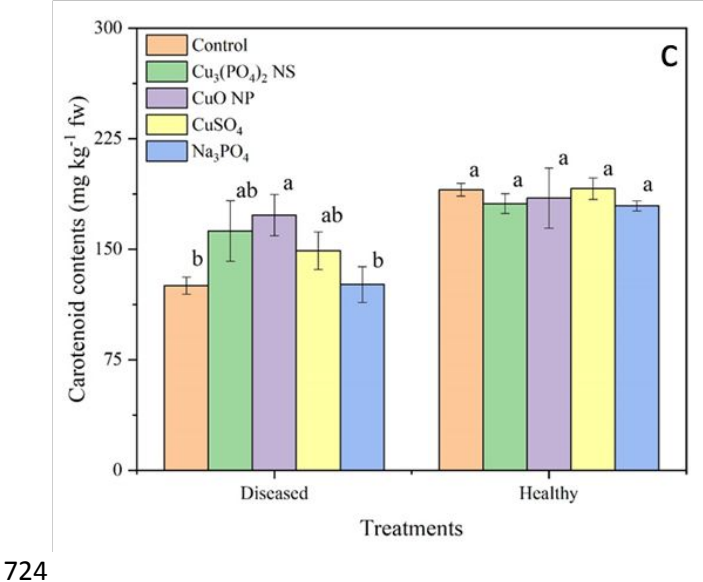
720

Figure 5. The total protein (a), PAL activity (b), POD activity (c) and PPO activity (d) of tomato roots in both diseased and healthy soil in greenhouse experiment.

(Note: NS, nanosheets; NP, nanoparticles; Bars with different letters are significantly different, and values are mean  $\pm$  S.D. (standard deviation); one-way ANOVA with Duncan's test (p < 0.05); fw, fresh weight).







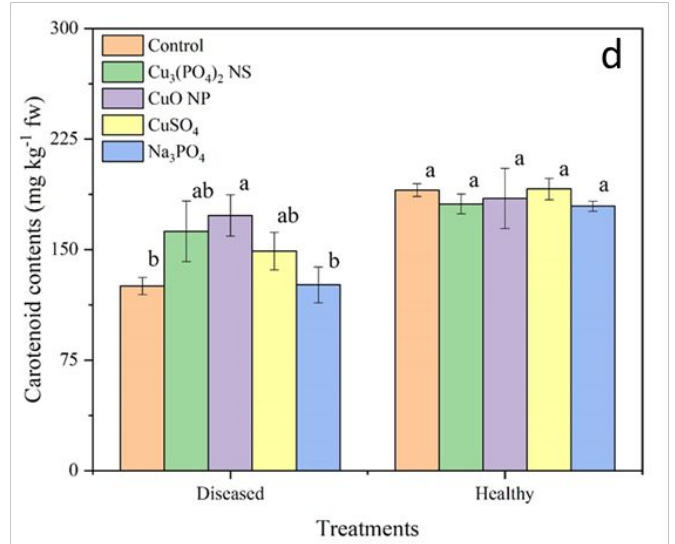


Figure 6. The chlorophyll a (a), chlorophyll b (b), carotenoid (c)and total chlorophyll content (d) of tomato shoots in both diseased and healthy soil in greenhouse experiment. Note: NS, nanosheets; NP, nanoparticles; Bars with different letters are significantly different, and values are mean  $\pm$  S.D. (standard deviation); one-way ANOVA with Duncan's test (p < 0.05); fw, fresh weight).

## **Table**

Table 1. Normalized cuticle content of Cu as a function of different treatments (CuO nanoparticles,  $Cu_3(PO_4)_2 \cdot 3H_2O$  nanosheets and  $CuSO_4$  solution) over time. For each Cu type, the data was normalized to the amount of Cu in the cuticle at 2, 4, 6 and 8 h.

	2 h	4 h	6 h	8 h
CuO nanoparticles	1.00 a	1.33 a	1.60 c	2.01 b
$Cu_3(PO_4)_2 \cdot 3H_2O$ nanosheets	1.00 a	1.22 a	1.67 b	0.85 c
Solubilized CuSO <sub>4</sub>	1.00 a	1.87 a	15.8 a	24.1 a

Note, different letters are significantly different; one-way ANOVA with Duncan's test (p < 0.05)